

CBPF-NF-011/82

TRIANGULAR AND HONEYCOMB LATTICES
BOND-DILUTED ISING FERROMAGNET:
CRITICAL FRONTIER

by

Aglaē C.N.de Magalhães, Georges Schwachheim
and Constantino Tsallis

TRIANGULAR AND HONEYCOMB LATTICES BOND-DILUTED
ISING FERROMAGNET: CRITICAL FRONTIER

by

Aglaē C.N. de MAGALHÃES,

Georges SCHWACHHEIM

and

Constantino TSALLIS

Centro Brasileiro de Pesquisas Físicas (CNPq)
Rua Xavier Sigaud, 150 - 22.290 - Rio de Janeiro
BRAZIL

ABSTRACT

Within a real space renormalization group framework (12 different procedures, all of them using star-triangle and duality-type transformations) we calculate accurate approximations for the critical frontiers associated with the quenched bond-diluted first-neighbour spin-1/2 Ising ferromagnet on triangular and honeycomb lattices. All of them provide, in both pure bond percolation and pure Ising limits, the exact critical points and exact or almost exact derivatives in the p - t space (p is the bond independent occupancy probability and $t \equiv \tanh J/k_B T$). Our best numerical proposals lead to the exact derivative in the pure percolation limit ($p = p_c$) and, in what concerns the pure Ising limit ($p = 1$) derivative, to a 0.15% error for the triangular lattice and to a 0.96% error for the honeycomb one; in the intermediate region ($p_c < p < 1$), where the exact critical frontiers are still unknown, the worst error in the t -variable (for fixed p) is estimated to be less than 0.27% for the triangular lattice and to a 0.14% for the honeycomb one. Furthermore we exhibit, on formal grounds, that the calculations of the exact critical points of the bond percolation and Ising models through the use of duality and star-triangle transformations can be unified within an appropriate graph framework.

I. INTRODUCTION

During the last few years, phase transitions in random magnetic systems have been studied by many authors. In particular, quite an effort has been dedicated to the discussion of the critical properties of the quenched bond-disordered Ising model using several approximate methods such as series expansions (Rappaport 1972, Harris 1974, Ditzian and Kadanoff 1979), Monte Carlo (Ono and Matsuoka 1976, Zobin 1978), variational method (Bidaux et al 1976), effective-interaction (Harris 1976, Turban 1980, Guilmin and Turban 1980) and effective-field (Tsallis et al 1982) approximations, duality and/or replica trick arguments (Lage 1977, Domany 1978, Oguchi and Ueno 1978, Sarbach 1980) and renormalization group (RG) techniques (Tatsumi and Kawasaki 1976, Jayaprakash et al 1978, Yeomans and Stinchcombe 1979, Tsallis and Levy 1980, Levy et al 1980, Chao et al 1981).

In the present work we shall consider the quenched bond-diluted first-neighbour spin-1/2 Ising ferromagnet on triangular and honeycomb lattices; the associated Hamiltonian is given by:

$$\mathcal{H} = - \sum_{\langle i,j \rangle} J_{ij} \sigma_i \sigma_j \quad (\sigma_i = \pm 1 \quad \forall i) \quad (1)$$

where $\langle i,j \rangle$ are nearest-neighbour sites and the bond strength J_{ij} is assumed to be an independent random variable with probability distribution.

$$P(J_{ij}) = (1-p)\delta(J_{ij}) + p\delta(J_{ij}-J) \quad (J>0) \quad (2)$$

Let us introduce the variable $t \equiv \tanh (J_{ij} / k_B T)$ (hereafter referred to as the thermal transmissivity of the bond) which appears naturally in spin-1/2 Ising problems (Domb 1960, Nelson and Fisher 1975, Young and Stinchcombe 1976, Yeomans and Stinchcombe 1979, Tsallis and Levy 1980 among others); the probability law (2) can be rewritten as follows:

$$P(t) \equiv P(t; p, t_0) = (1-p)\delta(t) + p\delta(t-t_0) \quad (3a)$$

$$\text{with } t_0 \equiv \tanh(J/k_B T) \quad (3b)$$

The exact para-ferromagnetic critical frontier (CF) for this model on triangular and honeycomb lattices is yet unknown; the only available exact results are the critical temperature for $p = 1$ (Wannier 1945), the critical probability p_c for $T = 0$ (Sykes and Essam 1963) and the derivatives $(dt_0/dp)_{p=1}$ and $(dt_0/dp)_{p=p_c}$ (Southern and Thorpe 1979) (upper and lower bounds on $t_0(p)$ (Bergstresser 1977) are known as well). As far as we know, all but one of the approximate CF's that have been proposed (Tatsumi and Kawasaki 1976, Oguchi and Ueno 1978, Yeomans and Stinchcombe 1979, Turban 1980, Guilmin and Turban 1980, Kinzel and Domany 1981) are not simultaneously exact at both pure limits; the unique exception is the three-bonds approximation of Guilmin and Turban (1980) (hereafter referred to as GT). They used a cluster extension of the effective interaction approximation where the effective medium was chosen to be that of a pure Ising model; this choice leads also to the exact derivative $(dt_0/dp)_{p=1}$. An accurate deter-

mination of the bond-diluted Ising CF on the triangular and honeycomb lattices constitutes the central aim of the present work. In section II we exhibit how the exact critical points in the pure limit cases can be recovered by using convenient graphs whose bonds are associated with transmissivities (for $p = 1$) or probabilities (for $t_0 = 1$). In section III we use these graphs (whose bonds are now associated with distribution laws) to construct 12 RG's which lead to accurate approximations for the bond-diluted Ising CF on the triangular lattice. We follow, in section IV, the same procedure to discuss the CF associated with the honeycomb lattice.

II. PURE MODELS EXACT RESULTS WITHIN AN UNIFIED GRAPH PROCEDURE

The star-triangle transformation (STT) (introduced by Onsager in 1944) and the duality transformation (DT) (introduced by Kramers and Wannier in 1941, interpreted geometrically by Onsager in 1944 and put in series-parallel terms by Tsallis and Levy 1980 and Alcaraz and Tsallis 1982) are the basic ingredients which, within different contexts, lead to the exact critical points $K_C^\Delta \equiv J/k_B T_C^\Delta$ and $K_C^Y \equiv J/k_B T_C^Y$ (Wannier 1945) of the pure Ising and p_C^Δ and p_C^Y (Sykes and Essam 1963) of the pure bond percolation models (Δ and Y respectively denote the triangular and honeycomb lattices). Let us briefly review the original arguments to obtain these points for let us say the triangular lattice. For the Ising model, Wannier (1945) established, through the STT (see Fig. 1), a connection between the partition function $Z_\Delta(K)$ of

the triangular lattice at a point K and the partition function $Z_Y(R)$ of the honeycomb lattice at the point $R = \arg \cosh [(1+e^{4K})/2]/2$. On the other hand, through the DT, he connected $Z_Y(R)$ to $Z_\Delta(K')$ where $K' = \arg \operatorname{coth} e^{2R} \equiv R^D$ (D stands for "dual"). In this way, Wannier derived a relation between the partition function Z_Δ of the triangular lattice at the points K and K' which, under the assumption of a single singularity in Z_Δ , leads to $K_C^\Delta = K = K' = (\ln 3)/4$. For the bond percolation problem, Sykes and Essam (1963) established, first, a relation (closely analogous to the above DT) between the high- and low-density series for the mean number of finite clusters per site; by assuming only one singular point they obtained $p_C^Y = (p_C^\Delta)^D \equiv 1 - p_C^\Delta$. Then, they considered a single star-triangle (for example, ABCO in Fig. 1) where the bonds of the triangle and those of the star have probabilities p and $p^D \equiv 1 - p$ respectively. By equating the connectivity on the triangle with that on the star, they arrived to an unique non-trivial independent equation (equivalent to eq.(j) of Table 1). The root of this equation is the exact critical probability $p_C^\Delta = 2\sin(\pi/18)$ (corresponding to the appearance of an infinite cluster on the triangular lattice).

Now, let us see how these exact critical points can be obtained within a compact and unified procedure by using graphs (see Tsallis and Levy 1981 and references therein). For the pure Ising model, Wannier's results can be recovered by considering the pair of two-terminal clusters shown in Fig. (a) of Table 1 ($i=2$) (or alternatively the pair of two-terminal graphs shown in Fig (b) of Table 1 ($i=2D$)) where we have introduced the

transmissivities $t_0 \equiv \tanh K$ and $r_0 \equiv \tanh R$. To be more precise, we associate $t_0(r_0)$ with each bond of the triangle (star) cluster of Fig (a) of Table 1 and obtain (see for example, Yeomans and Stinchcombe 1979, Tsallis and Levy 1981) the equivalent transmissivity $G_{\Delta}^{(2)}(t_0)$ ($G_Y^{(2)}(r_0)$) between the two terminal sites (see item (d) of Table 1). The standard STT (which involves a trace over the possible configurations of the central spin on the Y -cluster) leads to

$$\frac{t_0 + t_0^2}{1 + t_0^3} = r_0^2 \quad (4)$$

If we consider now that, on the critical point, $r_0 = t_0^D \equiv (1 - t_0) / (1 + t_0)$ we obtain the equation indicated in item (d) of Table 1. The procedure we have just outlined for the clusters appearing in Fig (a) of Table 1 can be also applied to those appearing in Fig (b) of Table 1 (these clusters are in fact the dual (Tsallis and Levy 1981) of the preceding ones) thus obtaining the equation indicated in item (e) of Table 1. For the pure bond percolation model, we can recover Sykes and Essam's results by considering the three-terminal ($i=3$) graphs shown in Fig (c) of Table 1, where p and p^D are the bond occupancy probabilities of the triangle and star clusters respectively. By equating the equivalent probabilities $G_{\Delta}^{(3)}(p)$ and $G_Y^{(3)}(p^D)$ between the terminals (i.e., the probabilities of the three terminals being connected) in both clusters, we obtain eq(j) of Table 1, whose root is the exact value p_c^{Δ} .

In other words, we have seen that the usual STT defined at the pure Ising critical point can be written in terms of

two-terminal graph pairs ($i=2$ or $2D$), while the usual STT defined at the pure bond percolation critical point can be written in terms of a three-terminal graph pair ($i=3$). Now, a natural question arises: could we obtain both exact critical points using the same pair of graphs? The answer is positive and we can verify that this is so for each graph pair ($i=2,2D,3$) we have considered in Table 1 (to obtain the equation indicated in item (f) of Table 1 we have used the Break-Collapse Method (Tsallis and Levy 1981)). More generally, it is easy to verify that this happens also for the pure anisotropic case even for $i = 2$ or $2D$ (where there is a break of permutation symmetry in the graphs). As a matter of fact, for the general anisotropic quenched random-bond Potts ferromagnetic model, the three-terminal graph pair ($i=3$) is the only one (among the three pairs herein considered) which leads to critical frontiers which do not violate (Tsallis 1982) the isomorphism (Kasteleyn and Fortuin 1969) existing between the $q \rightarrow 1$ Potts model and bond percolation. Therefore, for more general problems, the three-terminal star-triangle graph pair ($i=3$) is superior to any of the two-terminal graph pairs ($i=2,2D$).

Up to this point we have considered only the triangular lattice; the exact critical points for its dual lattice ($t_c^Y = (t_c^\Delta)^D = 1/\sqrt{3}$ and $p_c^Y = (p_c^\Delta)^D = 1 - 2\sin(\pi/18)$) can be derived similarly ditto with $\tau \leftrightarrow \tau^D$ ($\tau=t_0, p$).

III. TRIANGULAR LATTICE BOND-DILUTED ISING MODEL

III.1. Graph Method

The fact that the combined STT-DT defined at both pure limit cases $p = 1$ (eqs. appearing in items (d), (e) and (f) of Table 1) and $t_0 = 1$ (eqs. appearing in items (g), (h) and (j) of Table 1) can be expressed by the same graph pairs, allow us to generalize these results for any p and t_0 , thus obtaining approximations for the CF associated with the triangular lattice. To perform this we associate, with each bond of the graphs appearing in Table 1, the distributions $P(t)$ (eq.(3)) and $P^D(t)$ instead of τ and τ^D respectively, where the dual distribution $P^D(t)$ is given (Tsallis and Levy 1980) by

$$P^D(t) \equiv P^D(t;p,t_0) = \frac{2}{(1+t)^2} P(t^D;p,t_0) = (1-p)\delta(t-1) + p\delta(t-t_0^D) \quad (5)$$

The overall transmissivity distributions associated with the graphs shown in Figs (a), (b) and (c) of Table 1 are, respectively

$$P_{\Delta}^{(2)}(t) \equiv P_{\Delta}^{(2)}[P(t;p,t_0)] = p^3 \delta\left(t - \frac{t_0 + t_0^2}{1+t_0^3}\right) + p^2(1-p)\delta(t-t_0^2) \\ + [2p^2(1-p) + p(1-p)^2]\delta(t-t_0) + \left\{1 - [p^3 + 3p^2(1-p) + p(1-p)^2]\right\}\delta(t) \quad (6a)$$

$$P_Y^{(2)}(t) \equiv P_Y^{(2)}[P^D(t;p,t_0)] = p^2\delta[t-(t_0^D)^2] + 2p(1-p)\delta(t-t_0^D) + (1-p)^2\delta(t-1) \quad (6b)$$

$$\begin{aligned}
 P_Y^{(2D)}(t) &\equiv P_Y^{(2D)} [P^D(t;p,t_0)] = [P_{\Delta}^{(2)}(t)]^D = p^3 \delta \left[t - \frac{2(t_0^D)^2}{1+(t_0^D)^2} \right] \\
 &+ p^2(1-p) \delta \left(t - \frac{2t_0^D}{1+(t_0^D)^2} \right) + [2p^2(1-p) + p(1-p)^2] \delta(t-t_0^D) \\
 &+ [2p(1-p)^2 + (1-p)^3] \delta(t-1) \tag{6c}
 \end{aligned}$$

$$\begin{aligned}
 P_{\Delta}^{(2D)}(t) &\equiv P_{\Delta}^{(2D)} [P(t;p,t_0)] = [P_Y^{(2)}(t)]^D = p^2 \delta \left(t - \frac{2t_0}{1+t_0^2} \right) + 2p(1-p) \delta(t-t_0) \\
 &+ (1-p)^2 \delta(t) \tag{6d}
 \end{aligned}$$

$$\begin{aligned}
 P_{\Delta}^{(3)}(t) &\equiv P_{\Delta}^{(3)} [P(t;p,t_0)] = p^3 \delta \left(t - \frac{3t_0^2-t_0^3}{1+t_0^3} \right) + 3p^2(1-p) \delta(t-t_0^2) \\
 &+ \left\{ 1 - [p^3+3p^2(1-p)] \right\} \delta(t) \tag{6e}
 \end{aligned}$$

and

$$\begin{aligned}
 P_Y^{(3)}(t) &\equiv P_Y^{(3)} [P^D(t;p,t_0)] = p^3 \delta [t-(t_0^D)^3] + 3p^2(1-p) \delta [t-(t_0^D)^2] \\
 &+ 3p(1-p)^2 \delta(t-t_0^D) + (1-p)^3 \delta(t-1) \tag{6f}
 \end{aligned}$$

At this point, we use procedures similar to the second approach ("dual-type RG", which includes RG3 to RG6) introduced by Tsallis and Levy (1980) in the case of the square lattice bond-diluted Ising model. It consists in constructing RG's which renormalize $P_{\Delta}^{(i)}(t)$ into $P_Y^{(i)}(t) \equiv P_Y^{(i)} [P^D(t;p',t'_0)]$ ($i=2,2D$ or 3). Two different RG schemes are introduced herein, namely the dual-type canonical RG (CRG) and the dual-type parametric RG (PRG).

III.2. Dual-type Canonical Renormalization Groups (CRG)

The CRG treatment is similar to RG 4 of Tsallis and Levy (1980) and involves the calculation of flow lines and fixed points by the standard procedure (see, for example, Yeomans and Stinchcombe 1979). We construct six different CRG's which we denote by (r,i) -CRG ($r=t$ or s ; $i=2, 2D$ or 3), where s is defined below, r is the variable which is averaged and i refers to the corresponding star-triangle graph pair (see Table 1). Each (r,i) -CRG is defined through the following pair of equations:

$$\langle r \rangle_{P_{\Delta}^{(i)}} \equiv h_r^{(i)}(p, t_0) = \langle r \rangle_{P_Y^{(i)}} \equiv f_r^{(i)}(p', t_0'^D) \quad (7a)$$

$$\langle r^2 \rangle_{P_{\Delta}^{(i)}} \equiv k_r^{(i)}(p, t_0) = \langle r^2 \rangle_{P_Y^{(i)}} \equiv g_r^{(i)}(p', t_0'^D) \quad (7b)$$

$$(r = t, s; i = 2, 2D, 3)$$

where

$$s \equiv \frac{\ln(1+t)}{\ln 2} \quad (8)$$

and $\langle \dots \rangle_P$ denotes the average over a distribution P .

The variable s (Levy et al 1980, Tsallis 1981 a, Tsallis and de Magalhães 1981, de Magalhães and Tsallis 1981) is used here with the aim of obtaining the exact value of $(dt_0/dp)_{p=p_c^{\Delta}}$, as it was the case for the square lattice bond-diluted Ising model (Levy et al 1980). Observe that Eqs. (7) could be written as well in terms of the first - $(\kappa_1^{(r)}(P^{(i)})) \equiv \langle r \rangle_{P^{(i)}}$ and second-order

$(\kappa_2^{(r)}(P^{(i)})) \equiv \langle r^2 \rangle_{P^{(i)}} - (\langle r \rangle_{P^{(i)}})^2$ cumulants associated with $P^{(i)}(P^{(i)} = P_{\Delta}^{(i)} \text{ or } P_Y^{(i)})$, i.e., eqs. (7) are equivalent to $\kappa_1^{(r)}(P_{\Delta}^{(i)}) = \kappa_1^{(r)}(P_Y^{(i)})$ and $\kappa_2^{(r)}(P_{\Delta}^{(i)}) = \kappa_2^{(r)}(P_Y^{(i)})$.

Notice also that the eqs. which appear in Table 1 are particular cases ($p=p'=1$, $t_0=t'_0$ and $t_0=t'_0=1$, $p=p'$) of the system of eqs. (7). Therefore, all the CRG's contain the exact pure Ising point $(1, t_c^{\Delta})$ and the exact pure percolation point $(p_c^{\Delta}, 1)$ as fixed points. The flow-line joining these points provides, for each (r,i) -CRG, an approximation for the CF we are looking for (see Tables 2a and 3a). The $(s,2)$ and $(s,2D)$ -CRG's lead to the same CF due to special properties[†] of the s -variable and to the fact that $P_{\Delta}^{(2D)}(t) = [P_Y^{(2)}(t)]^D$ and $P_Y^{(2D)}(t) = [P_{\Delta}^{(2)}(t)]^D$. All these five distinct CF's are well represented by the curve (T) shown in Fig. 2a (or 2b) since their discrepancies (less than 1.1% in the t_0 -variable) are invisible within the scale of the figures.

Let us now discuss with more detail how the transformation equations (7) provide several critical properties of the present model, in particular the exact value of the derivative $(dt_0/dp)_{p=p_c^{\Delta}}$ in the (s,i) -CRG approximations. First of all, let us notice that the transmissivity distributions $(P_{\Delta}^{(i)}(t))$ and $(P_Y^{(i)}(t))$ ($i = 2, 2D, 3$) (see eqs. (6)) have the following general forms:

[†] These properties are $\kappa_1^{(s)}(P) = 1 - \kappa_1^{(s)}(P^D)$ and $\kappa_2^{(s)}(P) = \kappa_2^{(s)}(P^D)$ where P is an arbitrary distribution.

$$P_{\Delta}^{(i)}(t) = \alpha_0^{(i)}(p)\delta(t) + \sum_{\ell=1,2,\dots} \alpha_{\ell}^{(i)}(p)\delta[t - A_{\ell}^{(i)}(t_0)] \quad (9a)$$

(i = 2, 2D, 3)

$$P_Y^{(i)}(t) = \beta_0^{(i)}(p')\delta(t-1) + \sum_{\ell=1,2,\dots} \beta_{\ell}^{(i)}(p')\delta[t - B_{\ell}^{(i)}(t_0^D)] \quad (9b)$$

where $\alpha_1^{(i)}(p) = p^n$ (where n is the number of relevant bonds of the graph, hence $n = 2$ for eq.(6d) and $n = 3$ for eqs.(6a) and (6e)). The functions we have just defined have the following properties

$$\alpha_{\ell}^{(i)}(p=1) = \beta_{\ell}^{(i)}(p'=1) = \delta_{\ell,1} \quad (\text{Kronecker-delta}) \quad \ell = 0,1,\dots \quad (i = 2, 2D, 3) \quad (10a)$$

$$A_{\ell}^{(i)}(t_0=1) = 1 \quad \ell = 1,2,\dots \quad (i = 2, 2D, 3) \quad (10b)$$

$$B_{\ell}^{(i)}(t_0^D=0) = 0 \quad \ell = 1,2,\dots \quad (i = 2, 2D, 3) \quad (10c)$$

$$\sum_{\ell \geq 0} \alpha_{\ell}^{(i)}(p) = \sum_{\ell \geq 0} \beta_{\ell}^{(i)}(p) = 1 \quad \forall p \quad (i = 2, 2D, 3) \quad (10d)$$

These properties are of fundamental importance since they lead to many special results which we shall mention below.

From the transformation equations (7) we find, for each (r,i) -CRG ($r = t,s; i = 2, 2D, 3$), only two fixed points ($p' = p=p^*$, $t_0 = t_0' = t_0^*$) corresponding precisely to the already mentioned exact pure points. Linearizing these equations, for each (r,i) -CRG, around the percolation fixed point we obtain the

Jacobian matrix $\left. \frac{\partial(p', t_0')}{\partial(p, t_0)} \right|_{p^*=p_c^{\Delta}}^{(r,i)}$; its element $\left. \frac{\partial t_0'}{\partial p} \right|_{p^*=p_c^{\Delta}}^{(r,i)}$

vanishes due to the properties (10b) and (10c). Consequently, its eigenvalues are $(\partial p' / \partial p)_{p^* = p_c^\Delta}^{(r,i)} \equiv \lambda_p^{(r,i)}$ and $(\partial t'_0 / \partial t_0)_{p^* = p_c^\Delta}^{(r,i)}$; the eigenvectors are respectively horizontal and tangent to the CF (at the point $(p_c^\Delta, 1)$). To say it in other words, we have proved that the present recursive relations (eqs.(7)) provide along the p-axis the same eigenvalue the pure perco-

lation problem yields, i.e. $\lambda_p^{(r,i)} = \left(\frac{dh_r^{(i)}(p,1)}{dp} / \frac{df_r^{(i)}(p',0)}{dp'} \right)_{p^* = p_c^\Delta}$.

Furthermore it is easy to see that $\lambda_p^{(t,i)} = \lambda_p^{(s,i)} \equiv \lambda_p^{(i)}$ (for numerical values see Table 4). The slope of the CF at the percolation fixed point is given by

$$\left. \frac{dt_0}{dp} \right|_{p^* = p_c^\Delta}^{(r,i)} = \left[\left(\frac{\partial t_0^{(r,i)}}{\partial t_0} - \lambda_p^{(i)} \right) / \frac{\partial p'^{(r,i)}}{\partial t_0} \right]_{p^* = p_c^\Delta} \quad \text{which,}$$

for $r = t$, takes the particular value $(dt_0/dp)_{p^* = p_c^\Delta}^{(t,i)} = -3/2p_c^\Delta$ (see Table 2a). For the case $r = s$, it follows from (10b) and (10c) that

$$\left. \frac{dt_0}{dp} \right|_{p^* = p_c^\Delta}^{(s,i)} = (\ln 2) \left[\left(\frac{\partial t_0^{(t,i)}}{\partial t_0} - 2\lambda_p^{(i)} \right) / \frac{\partial p'^{(t,i)}}{\partial t_0} \right]_{p^* = p_c^\Delta} = -\frac{2 \ln 2}{p_c^\Delta},$$

which coincides with the exact result (Southern and Thorpe 1979).

At the Ising fixed point we can show, using property (10a), that $(\partial p' / \partial t_0)_{t^* = t_c^\Delta}^{(r,i)} = 0$. Therefore, the Jacobian matrix evaluated at this fixed point has eigenvalues $(\partial t'_0 / \partial t_0)_{t^* = t_c^\Delta}^{(r,i)} \equiv \lambda_t^{(r,i)}$ and $(\partial p' / \partial p)_{p^* = t_c^\Delta}^{(r,i)}$ associated respectively with the vertical eigenvector and with the eigenvector tangent to the CF

(at the point $(1, t_c^\Delta)$). Here again, the eigenvalue $\lambda_t^{(r,i)}$ is that of the

$$\text{pure case i.e., } \lambda_t^{(r,i)} = \left(\frac{dh_r^{(i)}(1, t_0)}{dt_0} / \frac{df_r^{(i)}(1, t_0^{D})}{dt_0'} \right)_{t^*=t_c^\Delta}$$

We verify also that $\lambda_t^{(t,i)} = \lambda_t^{(s,i)} \equiv \lambda_t^{(i)}$ (for numerical values see Table 4). The slope of the CF at the Ising fixed point, obtained through the (r,i) -CRG, is given by (Yeomans and Stinchcombe 1979)

$$\left. \frac{dt_0^{(r,i)}}{dp} \right|_{t^*=t_c^\Delta} = \left[\frac{\partial t_0^{(r,i)}}{\partial p} / \left(\frac{\partial p^{(r,i)}}{\partial p} - \frac{\partial t_0^{(r,i)}}{\partial t_0} \right) \right]_{t^*=t_c^\Delta} \quad (\text{see Table 2a for specific numerical values}).$$

2a for specific numerical values).

Let us notice that, within the dual-type RG framework, it is not possible to calculate approximations for the critical correlation length exponents $\nu_p^{(i)} = \ln b / \ln |\lambda_p^{(i)}|$ and $\nu_t^{(i)} = \ln b / \ln |\lambda_t^{(i)}|$ since, by construction, there is no expansion of the original cluster (linear expansion factor $b = B/B' = 1$, where B and B' are, respectively, the linear sizes of the Δ and Y -clusters) for all (r,i) -CRG.

We can see from Table 4 that $|\lambda_p^{(i)}(B=1)| \approx 1$ and $|\lambda_t^{(i)}(B=1)| \approx 1$ (within an error inferior to 6.5%), in particular, $|\lambda_t^{(2)}(B=1)| = |\lambda_t^{(2D)}(B=1)| = 1$.

The calculation of $|\lambda_p^{(i)}(B)|$ and $|\lambda_t^{(i)}(B)|$ in larger pairs (de Magalhães et al 1982) of Y - Δ clusters ($B = 2, 3$; a cluster with $B = 2$ is represented in Fig. 1) with i terminals ($i = 2$ to 6 for $B = 2$ and $i = 2$ to 10 for $B = 3$) shows that: i) for any cluster such that $(B,i) \neq (1,3)$, $|\lambda_p^{(i)}(B)| < |\lambda_p^{(3)}(1)|$ and $|\lambda_t^{(i)}(B)| < |\lambda_t^{(3)}(1)|$; ii) $|\lambda_t^{(2)}(B)| = 1$ for all values of B ; iii) the averages $|\lambda_p^{(i)}(B)|$ and $|\lambda_t^{(i)}(B)|$, taken over all clusters with the same number i of terminals and the same value for B , increase with increasing i (at fixed B) and decrease

with increasing B (at fixed i); iv) the averages $\overline{|\lambda_p^{(i)}(B)|}$ and $\overline{|\lambda_t^{(i)}(B)|}$, taken now over all clusters having the same B , approach to unity as B increases. All these tendencies strongly suggest that $|\lambda_p^{(i)}(B)| \rightarrow 1$ and $|\lambda_t^{(i)}(B)| \rightarrow 1$ as $B \rightarrow \infty$ ($\forall i$) leading consistently, as expected, to an indeterminacy in v_p and v_t , as it happened in the dual-type RG of Tsallis and Levy (1980).

The fact that there is no expansion of the lattice ($b = 1$) in all the (r,i) -CRG approximations, makes that no physical meaning can be associated with the senses of the dual-type RG flows.

III.3. Dual-type Parametric Renormalization Groups (PRG)

The parametric RG procedure (PRG) (RG 3 of Tsallis and Levy 1980, de Magalhães et al 1981, Chao et al 1981) provides, for CF's, results which are similar to the CRG ones and is considerably less harder to work out. It consists in solving equation (7a) for each (r,i) -PRG ($r = t,s; i = 2,2D,3$) by holding, during the considered renormalization transformation, a fixed parameter (e.g, $p, t_0, t_0/p$, etc), thus reducing the two-dimensional RG space to a one-dimensional one. In this way, each (r,i) -PRG approximation for the CF depends on the choice of the parameter and all of its points are fixed points (see de Magalhães et al 1981 for details).

The main results obtained through the present six (r,i) -PRG ($r = t,s; i = 2,2D,3$) are indicated in Tables (2a) and (3a). Let us stress that all (s,i) -PRG ($i = 2,2D,3$) lead to one and the same approximation for the CF, namely

$$3p \ln(1+t_0) - p^3 \ln(1+t_0^3) - \ln 2 = 0 \quad (11)$$

whose slope at the percolation fixed point is exact (Eq. (11) provides in fact an excellent and simple analytic approximation for the CF). The PRG approximations for the CF differ very little among them (the maximum discrepancy in t_0 occurs in $p \approx 0.45$ and is about 0.65%) and are, as it was the case of the CRG approximations, well represented by the curve (T) drawn in Fig. (2a) (or 2b).

III.4. Comparisons

Guilmin and Turban (1980) derived, within their "three-bonds" approximation (GT), a CF which contains both exact pure points and the exact derivative $(dt_0/dp)_{p=1}$. We have calculated, in the GT approximation, the other derivative and have obtained that $(-dt_0/dp)_{p=p_c^\Delta} = 12(1+p_c^\Delta) / [p_c^\Delta(9+7p_c^\Delta)] \approx 4.0725$ (see Table 2a). For comparison, we have calculated (Table 3a) a few points of their CF.

All the approximate CF's we have considered up to now ((r,i)-CRG, (r,i)-PRG and GT; $r = t, s$; $i = 2, 2D, 3$) are very close among them (the difference in t_0 being about 2% in the most unfavourable case); they are represented by the same curve within the scales of Figs. (2a) and (2b). All the s-RG's lead to the exact value of $(dt_0/dp)_{p=p_c^\Delta}$ (cf Table 2a). Notice that the PRG CF's are, in the p - t_0 space, a little above the CRG ones, as it was the case for the square (Tsallis and Levy 1980) and SC (Chao et al 1981) lattices. Since the exact CF $t_0(p)$ is a monotonically

function of p (Bergstresser 1977), and presumably the derivative dt_0/dp also, the analysis of the pure cases derivatives suggests that the unknown exact CF lies between the GT approximation (lower bound for t_0 ; 2% error in $(dt_0/dt)_{p=p_c^\Delta}$) and our (s,3)-CRG one (upper bound for t_0 ; 0.15% error in $(dt_0/dp)_{p=1}$); see the numbers within the heavy line in Table 3a. The maximum discrepancy (in t_0) between the GT and (s,3)-CRG curves occurs at $p \approx 0.45$ and is close to 0.002 (which implies in a percentual discrepancy of 0.27%)

IV. HONEYCOMB LATTICE BOND-DILUTED ISING MODEL

IV.1. Graph Method

For the honeycomb lattice, the distribution law $P(t)$ (eqs.3) is now associated with each bond of the i -terminal Y -clusters ($i = 2, 2D$ or 3) and its dual $P^D(t)$ is associated with each bond of the corresponding Δ -clusters (i.e., substitute τ^D by $P(t)$ and τ by $P^D(t)$ in Figs (a), (b) and (c) of Table 1). Following the same procedure and notation of sub-section III-1, we obtain the equivalent transmissivity distributions associated with the graphs shown in Figs. (a), (b) and (c) of Table 1:

$$P_{\Delta}^{(2)}(t) \equiv P_{\Delta}^{(2)} [P^D(t;p,t_0)] = p^3 \delta \left[t - \frac{t_0^D + t_0^{D^2}}{1 + (t_0^D)^3} \right] + 2p^2(1-p) \delta \left[t - \frac{2t_0^D}{1 + (t_0^D)^2} \right] +$$

$$+ \left\{ 1 - [p^3 + 2p^2(1-p)] \right\} \delta(t-1) \quad (12a)$$

$$P_Y^{(2)}(t) \equiv P_Y^{(2)} [P(t;p,t_0)] = p^2 \delta(t-t_0^2) + (1-p^2) \delta(t) \quad (12b)$$

$$P_Y^{(2D)}(t) \equiv P_Y^{(2D)} [P(t;p,t_0)] = [P_Y^{(2)}(t)]^D = p^3 \delta \left[t - \frac{2t_0^2}{1+t_0^2} \right] + 2p^2(1-p) \delta(t-t_0^2) \\ + \left\{ 1 - [p^3 + 2p^2(1-p)] \right\} \delta(t) \quad (12c)$$

$$P_{\Delta}^{(2D)}(t) \equiv P_{\Delta}^{(2D)} [P^D(t;p,t_0)] = [P_Y^{(2)}(t)]^D = p^2 \delta \left[t - \frac{2t_0^D}{1+(t_0^D)^2} \right] \\ + [2p(1-p) + (1-p)^2] \delta(t-1) \quad (12d)$$

$$P_{\Delta}^{(3)}(t) \equiv P_{\Delta}^{(3)} [P^D(t;p,t_0)] = p^3 \delta \left[t - \frac{3(t_0^D)^2 - (t_0^D)^3}{1+(t_0^D)^3} \right] + 3p^2(1-p) \delta \left[t - \frac{2t_0^D}{1+(t_0^D)^2} \right] \\ + \left\{ 1 - [p^3 + 3p^2(1-p)] \right\} \delta(t-1) \quad (12e)$$

$$P_Y^{(3)}(t) \equiv P_Y^{(3)} [P(t;p,t_0)] = p^3 \delta(t-t_0^3) + (1-p^3) \delta(t) \quad (12f)$$

Using these distributions we construct, similarly to the previous section, twelve RG's which renormalize $P_Y^{(i)}(t)$ into $P_{\Delta}^{(i)}(t) \equiv P_{\Delta}^{(i)} [P^D(t;p',t_0^D)]$ ($i = 2, 2D$ or 3).

IV.2. Dual-type Canonical Renormalization Groups (CRG)

Similarly to subsection (III-2), each (r,i) -CRG ($r = t, s$; $i = 2, 2D, 3$) is defined by the following system of equations:

$$\langle r \rangle_{P_Y^{(i)}} \equiv \bar{h}_r^{(i)}(p, t_0) = \langle r \rangle_{P_{\Delta}^{(i)}} \equiv \bar{f}_r^{(i)}(p', t_0^D) \quad (13a)$$

$$\langle r^2 \rangle_{p(i)}^Y \equiv \bar{k}_r^{(i)}(p, t_0) = \langle r^2 \rangle_{p'_\Delta(i)} \equiv \bar{g}_r^{(i)}(p', t_0^D) \quad (13b)$$

(r = t, s; i = 2, 2D, 3)

The flow lines associated with these equations lead to five distinct CF's (since the (s,2) and (s,2D) ones are numerically identical as it was the case for the triangular lattice) which differ so little among them (less than 0.8% in the t_0 -variable) that they are represented, within the scale of Fig. (2a) (or (2b)), by one and the same curve (H); their derivatives at the exact pure points $(1, t_c^Y)$ and $(p_c^Y, 1)$ and a few points of the approximate CF's are respectively reported in Tables (2b) and (3b).

Since relations (9) and (10) are still valid ditto with $\Delta \nleftrightarrow Y$, all their consequences (mentioned in subsection (III-2)) still hold. Taking into account that the pure case equations for the honeycomb lattice can be obtained from the corresponding ones for the triangular lattice by simply replacing $\tau \nleftrightarrow \tau^D$ ($\tau=p, t_0$), one can easily show that $\lambda_p^{(i)\Delta} \lambda_p^{(i)Y} = \lambda_t^{(i)\Delta} \lambda_t^{(i)Y} = 1$ ($i = 2, 2D, 3$) (see Table 4 for numerical values of the λ 's). The senses of flow along each (r,i)-CRG approximation for the CF, as well as the spurious fixed points (see Table 2b) which appear in the three (s,i)-CRG's ($i = 2, 2D, 3$) are physically meaningless (due to the fact that $b = 1$). At first glance, it might strike the fact that the topology of the set of CF's (e.g., the number of intersections among them and the number of fixed points) associated to the honeycomb lattice is different from that of the triangular lattice (compare Tables 3a and 3b). This is due to the fact that we are considering a restricted problem (bond-di-

luted instead of bond-mixed): the overall symmetry should appear if we had assumed $P(t) = (1-p)\delta(t-t_1) + p\delta(t-t_0)$ instead of eq. (3a).

IV.3. Dual-type Parametric Renormalization Groups (PRG)

Similarly to sub-section (III-3), we obtain the (r,i) -PRG ($r = t,s; i = 2,2D,3$) CF's through the line of fixed points associated with transformation (13a). In the case of $r = s$, it leads, as before, to the same equation for all three (s,i) -PRG ($i = 2,2D,3$) CF's, namely

$$3p^2(1-p)\ln(1+t_0^2) + p^3\ln(1+3t_0^2) - \ln 2 = 0 \quad (14)$$

which provides the exact derivative $(dt_0/dp)_{p=p_c^Y}$ (eqs. (14) is an excellent and simple analytic approximation for the CF). The PRG approximate CF's are very close among them (the discrepancy in t_0 being inferior to 0.41%) and are represented by the curve (H) shown in Fig. (2a) (or (2b)); the main results and some intermediate points are respectively reported in Tables 2b and 3b.

IV.4. Comparisons

In the GT approximation for the CF, the extreme points and the derivative $(dt_0/dp)_{p=1}$ are exact. We have calculated, in

the GT approximation, the other derivative and have obtained $-(dt_0/dp)_{p=p_c^Y} = 6(2-p_c^Y)/[p_c^Y(9-5p_c^Y)] \approx 2.1590$ (see Table 2b). For comparison, we have also calculated (Table 3b) a few points of their CF.

Similarly to the triangular case, all the CF's (CRG's, PRG's and GT approximations) differ very little one from the other (less than 1.3% in the t_0 variable) and their graphical representations reduce to one and the same curve (H) within the scales of Figs. (2a) and (2b). In all s-RG's, the value of $(dt_0/dp)_{p=p_c^Y}$ is the exact one (see Table 2b). Here again (as in section III), the values of t_0 , for any fixed p , along the PRG CF's are a little higher than along the CRG ones. The analysis of the extreme derivatives (Table 2b) suggests that the unknown exact CF lies between the (s,2)-CRG curve (upper bound for t_0 ; 0.96% error in $(dt_0/dp)_{p=1}$) and a curve (lower bound for t_0 ; no error in the pure cases derivatives) which is made, for $p_c^Y \leq p \lesssim 0.90$, by the (s,3)-CRG one and, for $0.90 \lesssim p \leq 1$, by the GT one (see the region of Table 3b delimited by a heavy line). The maximum discrepancy in t_0 between the upper and lower bounds occurs at $p \approx 0.90$ and its value is close to 0.001 (which implies a percentual discrepancy of 0.14%).

V. CONCLUSION

We exhibit that the duality and star-triangle transformations, which enable the calculation of the exact pure Ising and bond percolation critical points, can be formulated within an unified

graph framework (it is possible to simultaneously obtain both exact critical points by using a single star-triangle pair of graphs, and we have herein illustrated this statement through 3 different such pairs). This fact allowed us to construct, within a real space renormalization group framework, 12 different procedures to calculate the critical frontiers associated with the quenched bond-diluted spin-1/2 first-neighbour interaction ferromagnetic Ising model on triangular and honeycomb lattices. We obtained 9 different accurate approximate critical frontiers (which differ, in the t_0 variable, by less than 2%) for the triangular lattice, and another 9 different approximate critical frontiers (which differ, in the t_0 variable, by less than 1.3%) for the honeycomb lattice. All these critical frontiers contain the exact pure Ising and bond percolation critical points as well as the exact or almost exact derivatives (in the p - t_0 space) at both pure limits.

On analytical grounds we propose for both lattices excellent and simple approximate critical frontiers, both exact in what concerns the derivative $(dt_0/dp)_{p=p_c}$. The triangular lattice proposal (eq. 11) provides a 0.40% error in the derivative $(dt_0/dp)_{p=1}$ and a maximum error (in $p \approx 0.45$) estimated to be about 0.31% in the t_0 variable. The honeycomb lattice proposal (Eq. 14) provides a 1.4% error in the derivative $(dt_0/dp)_{p=1}$, and a maximum error (in $p \approx 0.90$) estimated to be about 0.14% in the t_0 -variable.

On numerical grounds, it has been possible to obtain even more precise approximations. The unknown exact critical frontier for the triangular lattice very probably lies between the pre

sent (s,3)-CRG approximation (exact $(dt_0/dp)_{p=p_c^\Delta}$ and 0.15% error in $(dt_0/dp)_{p=1}$) and Guilmin and Turban (1980) "three-bonds" approximation (exact $(dt_0/dp)_{p=1}$ and 2% error in $(dt_0/dp)_{p=p_c^\Delta}$); their highest discrepancy achieves 0.27% at $p \approx 0.45$. The bounds for the honeycomb lattice critical frontier are the present (s,2)-CRG approximation (exact $(dt_0/dp)_{p=p_c^Y}$ and 0.96% error in $(dt_0/dp)_{p=1}$) and a curve which, for $p_c^Y \leq p \lesssim 0.90$, coincides with the present (s,3)-CRG approximation (exact $(dt_0/dp)_{p=p_c^Y}$) and, for $0.90 \lesssim p \leq 1$, coincides with Guilmin and Turban (1980) "three-bonds" approximation (exact $(dt_0/dp)_{p=1}$); their biggest discrepancy achieves 0.14% at $p \approx 0.90$. To the best of our knowledge, the present bounds for the unknown exact critical frontiers for the triangular and honeycomb lattices are the tightest available in the literature; therefore the real space renormalization group methods can be extremely efficient in what concerns critical frontiers whenever convenient lattice symmetries (and transformations) can be introduced.

ACKNOWLEDGMENTS

We acknowledge L. Turban for communicating to us unpublished details concerning the paper Guilmin and Turban 1980.

REFERENCES

- Alcaraz FC and Tsallis C, 1982, J. Phys. A: Math. Gen. 15, 587-98
- Bergstresser TK, 1977, J. Phys. C: Solid St. Phys. 10, 3831-49
- Bidaux R, Carton JP and Sarma G, 1976, J. Phys. A: Math. Gen 9, L87-91
- Chao NC, Schwachheim G and Tsallis C, 1981, Z. Phys. B43, 305-13
- Ditzian RV and Kadanoff LP, 1979, Phys. Rev. B19, 4631-45
- Domany E, 1978, J. Phys. C: Solid St. Phys. 11, L337-42
- Domb C, 1960, Adv. Phys. 9, 149-361
- Guilmin P and Turban L, 1980, J. Phys. C: Solid St. Phys. 13, 4077-89
- Harris AB, 1974, J. Phys. C: Solid St. Phys. 7, 1671-92
- Harris AB, 1976, J. Phys. C: Solid St. Phys. 9, 2515-8
- Jayaprakash C, Riedel EK and Wortis M, 1978, Phys. Rev. B18, 2244-55
- Kasteleyn PW and Fortuin CM, 1969, J. Phys. Soc. Japan Suppl. 26, 11-4
- Kinzel W and Domany E, 1981, Phys. Rev. B23, 3421-34
- Kramers HA and Wannier GH, 1941, Phys. Rev. 60, 252-62
- Lage EJS, 1977, J. Phys. C: Solid St. Phys. 10, 701-18
- Levy SVF, Tsallis C and Curado EMF, 1980, Phys. Rev. B21, 2991-8
- Magalhães ACN de, Tsallis C and Schwachheim G, 1981, J. Phys. C: Solid St. Phys. 14, 1393-408
- Magalhães ACN de and Tsallis C, 1981, J. Physique 42, 1515-23
- Magalhães ACN de, Tsallis C. and Schwachheim G, 1982, to be published
- Nelson DR and Fisher ME, 1975, Ann. Phys. 91, 226-74
- Oguchi T and Ueno Y, 1978, J. Phys. Soc. Japan 44, 1449-54
- Ono I and Matsuoka Y, 1976, J. Phys. Soc. Japan 41, 1425-6
- Ønsager L, 1944, Phys. Rev. 65, 117-49
- Rappaport DC, 1972, J. Phys. C: Solid St. Phys. 5, 1830-58; J. Phys. C: Solid St. Phys. 5, 2813-26
- Sarbach S, 1980, J. Phys. C: Solid St. Phys. 13, 5033-57; J. Phys. C: Solid St. Phys. 13, 5059-70

- Southern BW and Thorpe MF, 1979, J. Phys. C: Solid St. Phys. 12, 5351-60
- Sykes MF and Essam JW, 1963, Phys. Rev. Lett. 10, 3-4
- Tatsumi T and Kawasaki K, 1976, Prog. Theor. Phys. 55, 612-5
- Tsallis C, 1981 a, J. Phys. C: Solid St. Phys. 14, L85-91
- 1981b, Kinam/Revista de Física (Mexico) 3, 79-118
- 1982, to be published
- Tsallis C, Fittipaldi IP and Sarmento EF, 1982, to be published
- Tsallis C and Levy SVF, 1980, J. Phys. C: Solid St. Phys. 13, 465-70
- 1981, Phys. Rev. Lett. 47, 950-3
- Tsallis C and Magalhães ACN de, 1981, J. Physique Lett. 42, L227-31
- Turban L, 1980, Phys. Lett. 75A, 307-10
- Wannier GH, 1945, Rev. Mod. Phys. 17, 50-60
- Yeomans JM and Stinchcombe RB, 1979, J. Phys. C: Solid St. Phys. 12, 347-60
- Young AP and Stinchcombe RB, 1976, J. Phys. C: Solid St. Phys. 9, 4419-31
- Zobin D, 1978, Phys. Rev. B18, 2387-90

CAPTIONS FOR FIGURES AND TABLES

Fig. 1 Illustration of the star-triangle overlapping of the triangular and honeycomb lattices in a cluster of linear size $B = 2$.

Fig. 2 Full curves represent the para (P) - ferro (F) magnetic critical frontiers for the bond-diluted Ising model on the triangular (T) and the honeycomb (H) lattices obtained through (r,i) -CRG or (r,i) -PRG ($r=t,s; i=2,2D,3$) or through the three-bonds approximation of Guilmin and Turban (1980) (all these curves are indistinguishable within the present scales); broken curves represent rigorous upper and lower bounds (Bergstresser 1977). (a) $p - t_0$ space; (b) $p - T$ space.

TABLE 1 Three graph representations of the star-triangle (ST) and duality (D) transformations for the pure Ising and pure bond percolation models on the triangular lattice. The solid (open) circles denote the internal sites (terminal sites) (see, for example, Tsallis and Levy 1981). (a) pair of two-terminal ($i=2$) clusters and their corresponding graphs; (b) two-terminal graphs ($i=2D$) obtained by application of duality on the graphs shown in item (a); (c) three-terminal graphs (or clusters) ($i=3$). $G_{\Delta}^{(i)}(\tau)$ and $G_{\Upsilon}^{(i)}(\tau)$ ($\tau=t_0$ or p ; $i=2,2D$ or 3) stand for the equivalent transmissivities ($\tau=t_0$) or probabilities ($\tau=p$) between the terminal sites of the corresponding i -terminal ($i=2,2D$ or 3) graphs. The exact

critical points of the pure Ising ($t_0^\Delta = 2 - \sqrt{3}$) and the pure bond percolation ($p^\Delta = 2\sin\pi/18$) models on the triangular lattice are roots of Eqs. (d)-(j). Eq. (j) also appears in Tsallis 1981b; eqs. (j) and (f) are particular cases ($q=1,2; t_1=t_2=t_3$) of the anisotropic Potts critical frontier considered by Tsallis and Levy (1981). A similar table holds for the honeycomb lattice ditto with $\tau \rightleftharpoons \tau^D$ ($\tau=p, t_0$) and $\Delta \rightleftharpoons Y$; therefore, the exact critical points of the pure Ising ($t_0^Y = (t_0^\Delta)^D = 1/\sqrt{3}$) and the pure bond percolation ($p^Y = (p^\Delta)^D = 1 - 2\sin\pi/18$) models on the honeycomb lattice are roots of the corresponding equations of the referred table.

TABLE 2 Main derivatives associated with the present RG's and with the three-bonds approximations of Guilmin and Turban (1980) (GT), as well as the exact ones (Southern and Thorpe 1979) for the Ising model on the triangular (a) and honeycomb (b) lattices. All of these approximations contain the exact critical points in the pure Ising and bond percolation limits. The numerical values for $-(dt_0/dp)_{p=p_c}$ decrease monotonically from the top to the last row. (*) indicates that the sense of the flow is from the percolation fixed point to the Ising fixed point while (**) indicates that the flow has a reserved sense; in the case of the honeycomb lattices appears a spurious fixed point $((p, t_0) \approx (0.705, 0.900))$

in the (s,2) and (s,2D)-CRG's and (0.707, 0.897) in the (s,3)-CRG) in the mid-region of the critical line which is unstable (+) or stable (++) along the critical line.

TABLE 3 Critical transmissivities (t_0) (for selected values of p) obtained through the present RG's and through the three-bonds approximation of Guilmin and Turban(1980) (GT) associated with the triangular (a) and honeycomb (b) lattices. Some of these approximations present intersections (p_{int}) in the mid-region: in (a) there is only one such point $p_{int} \approx 0.45$ originated from the last two PRG's, while in (b) there are six intersection points, for example, the (s,3)-CRG curve intersects both GT and (t,2D)-CRG curves in $p_{int} \approx 0.90$ and 0.94 respectively. The sequence of approximations are ordered, from the top to the bottom, according to the increasing values of t_0 for a fixed $p \in [p_c, p_{int}]$; (...) denotes an exact value. The values of t_0 , for fixed p , corresponding to the unknown exact critical frontier very probably lie between the ones enclosed by a heavy line.

TABLE 4 Approximate eigenvalues of the Jacobian matrix calculated in the (t or s,i)-CRG approximations (i=2,2D,3) for the triangular (Δ) and honeycomb (Y) lattices. $\lambda_p^{(i)}$ and $\lambda_t^{(i)}$ are respectively associated with the horizontal eigenvector at ($p_c, 1$) and with the vertical

eigenvector at $(1, t_c)$. Observe that $\lambda_p^{(2D)} = [\lambda_p^{(2)}]^{-1}$ and $\lambda_t^{(2D)} = [\lambda_t^{(2)}]^{-1}$ for both lattices (these facts follow from the property $\langle s \rangle_p = 1 - \langle s \rangle_{p^D}$).

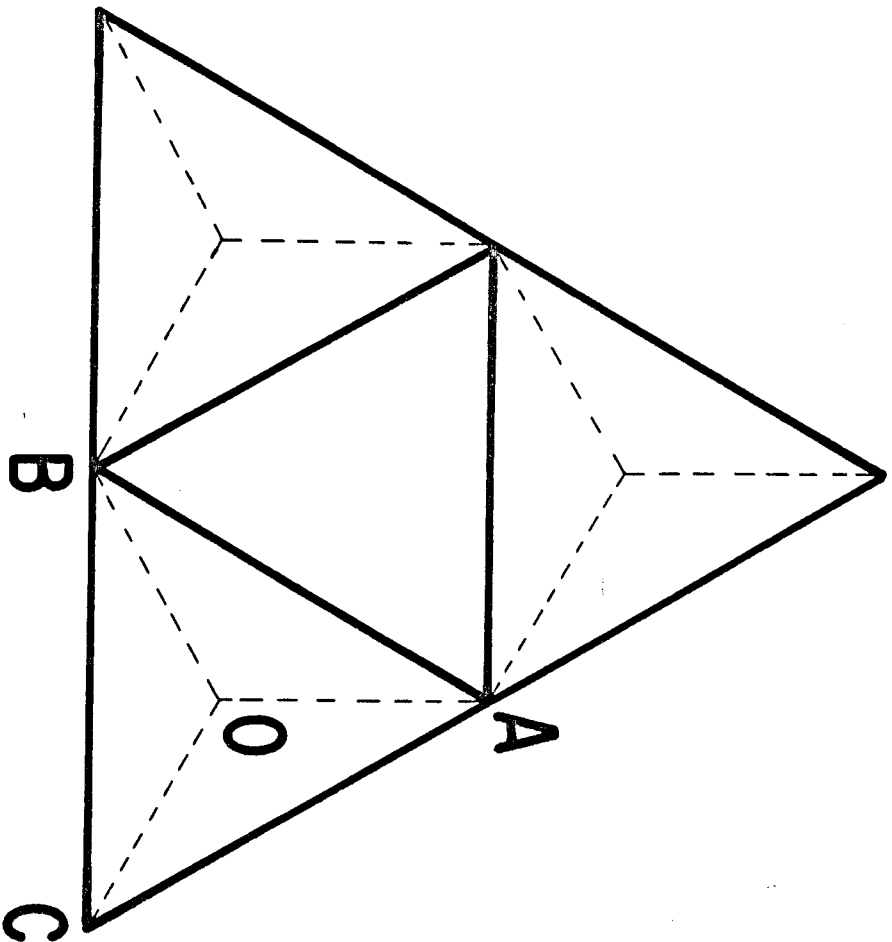


FIG.1

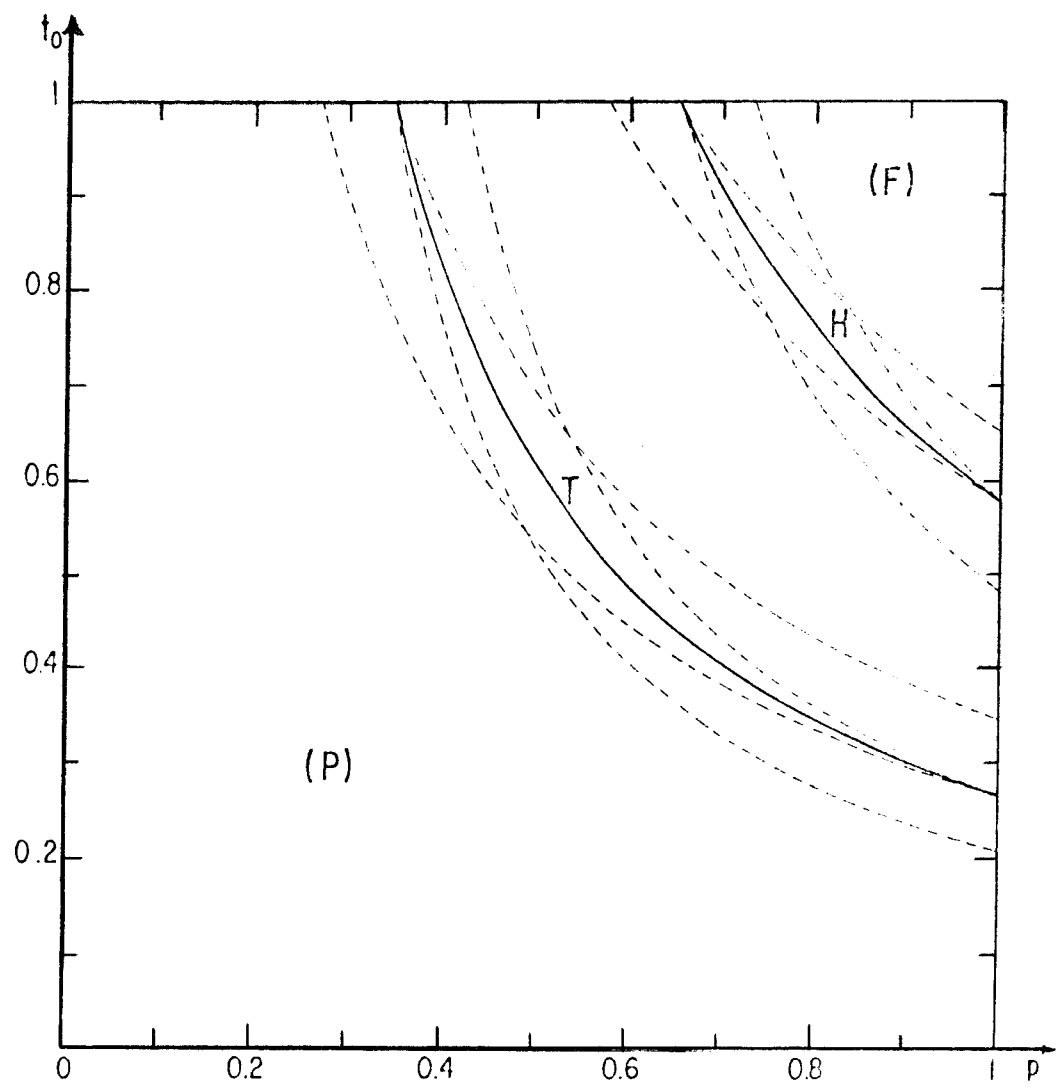


FIG. 2a

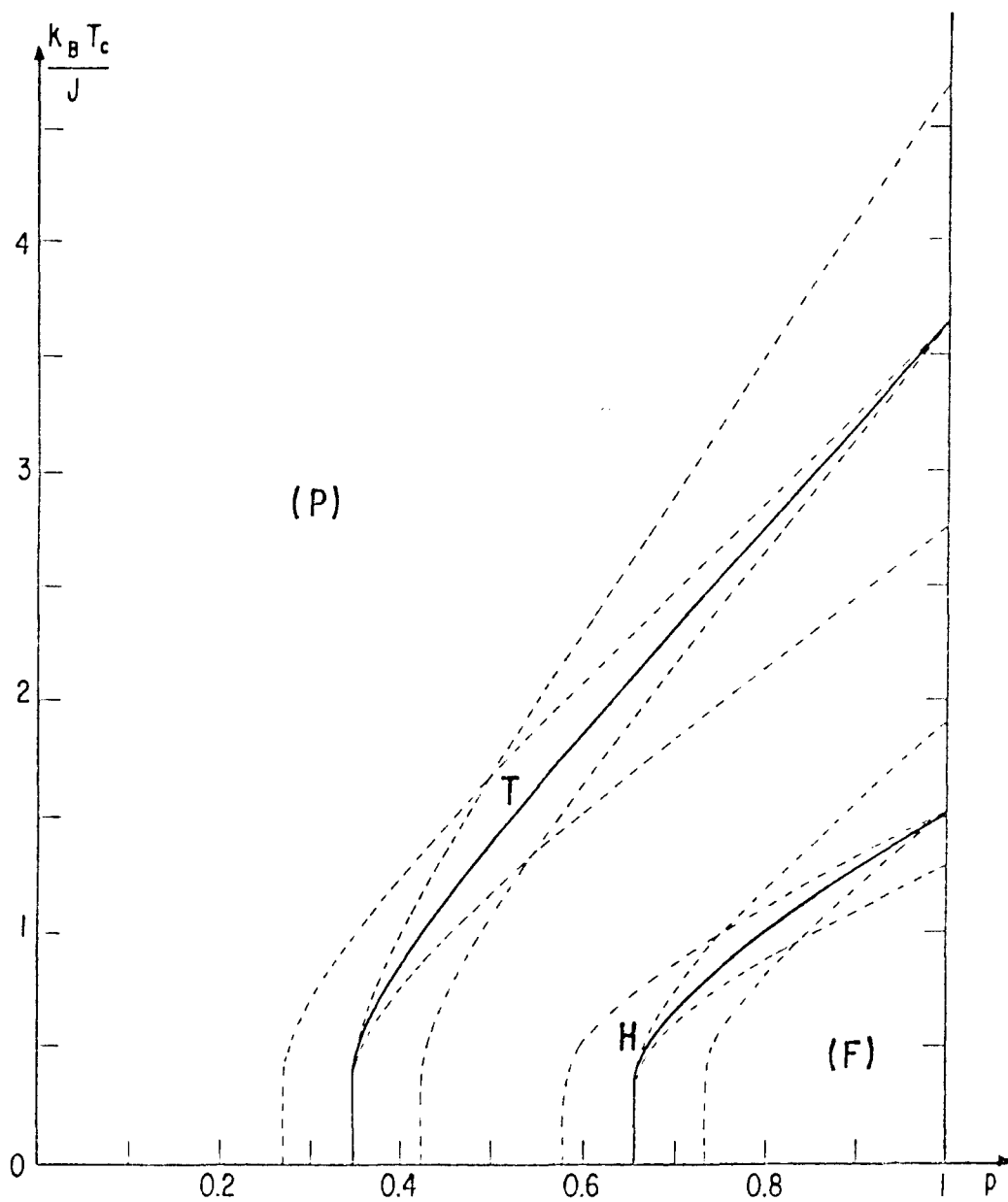


FIG. 2b

TABLE 1

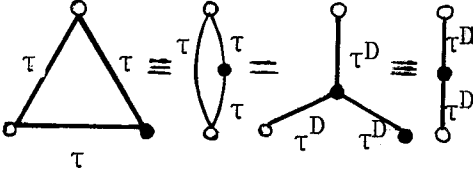
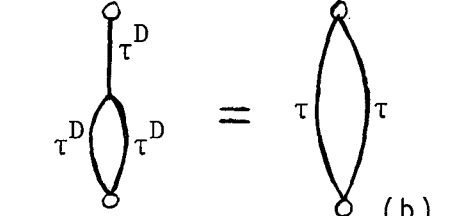
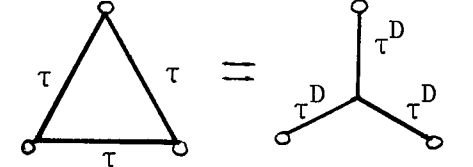
i	ST-D graph transformations	$\tau = t_0$	$\tau = p$
2	 <p>(a)</p>	$G_{\Delta}^{(2)}(t_0) \equiv \frac{t_0 + t_0^2}{1 + t_0^3} = (t_0^D)^2 \equiv G_Y^{(2)}(t_0^D)$ <p>(d)</p>	$G_{\Delta}^{(2)}(p) \equiv p + p^2 - p^3 = (p^D)^2 \equiv G_Y^{(2)}(p^D)$ <p>(g)</p>
2D	 <p>(b)</p>	$G_Y^{(2D)}(t_0^D) \equiv \frac{2(t_0^D)^2}{1 + (t_0^D)^2} = \frac{2t_0}{1 + t_0^2} \equiv G_{\Delta}^{(2D)}(t_0)$ <p>(e)</p>	$G_Y^{(2D)}(p^D) \equiv 2(p^D)^2 - (p^D)^3 = 2p - p^2 \equiv G_{\Delta}^{(2D)}(p)$ <p>(h)</p>
3	 <p>(c)</p>	$G_{\Delta}^{(3)}(t_0) \equiv \frac{3t_0^2 - t_0^3}{1 + t_0^3} = (t_0^D)^3 \equiv G_Y^{(3)}(t_0^D)$ <p>(f)</p>	$G_{\Delta}^{(3)}(p) \equiv 3p^2 - 2p^3 = (p^D)^3 \equiv G_Y^{(3)}(p^D)$ <p>(j)</p>

TABLE 2a

method	$-\frac{dt_0}{dp} \Big _{p=p_c^\Delta} = 2 \frac{d}{dp} e^{-2\beta J} \Big _{p=p_c^\Delta}$	$-\frac{dt_0}{dp} \Big _{p=1}$	$\frac{1}{T_c} \frac{dT_c}{dp} \Big _{p=1}$
(t,2)-CRG ^(*)	4.3191	0.2993	1.1739
(t,3)-CRG ^(*)	4.3191	0.3003	1.1779
(t,2D)-CRG ^(*)	4.3191	0.3021	1.1849
GT	4.0725	$6(30-17\sqrt{3})/11 \approx 0.3028$	$12(3\sqrt{3}-4)/11 \ln 3 \approx 1.1878$
exact	$2 \ln 2 / p_c^\Delta \approx 3.9917$	$6(30-17\sqrt{3})/11 \approx 0.3028$	$12(3\sqrt{3}-4)/11 \ln 3 \approx 1.1878$
(s,3)-CRG ^(*)	$2 \ln 2 / p_c^\Delta \approx 3.9917$	0.3032	1.1895
$\left\{ \begin{array}{l} (s,2)-CRG^{(*)} \\ (s,2D)-CRG^{(**)} \end{array} \right.$	$2 \ln 2 / p_c^\Delta \approx 3.9917$	0.3037	1.1914
(s,i)-PRG (i = 2,2D,3)	$2 \ln 2 / p_c^\Delta \approx 3.9917$	0.3040	1.1925
(t,2D)-PRG	3.8525	0.3047	1.1952
(t,2)-PRG	3.8260	0.3064	1.2020
(t,3)-PRG	3.7998	0.3054	1.1978

TABLE 2b

method	$-\frac{dt_0}{dp} \Big _{p=p_c} = 2 \frac{d}{dp} e^{-2\beta J} \Big _{p=p_c}$	$-\frac{dt_0}{dp} \Big _{p=1}$	$\frac{1}{T_c} \frac{dT_c}{dp} \Big _{p=1}$
(t,2)-CRG ^(*)	2.2981	0.6662	1.5175
(t,3)-CRG ^(*)	2.2981	0.6623	1.5088
(t,2D)-CRG ^(*)	2.2981	0.6902	1.5722
GT	2.1590	$2\sqrt{3}/5 \approx 0.6928$	$6\sqrt{3}/[5\ln(2+\sqrt{3})] \approx 1.578$
(s,3)-CRG ⁽⁺⁾	$2\ln 2/p_c^Y \approx 2.1239$	0.6839	1.5579
exact	$2\ln 2/p_c^Y \approx 2.1239$	$2\sqrt{3}/5 \approx 0.6928$	$6\sqrt{3}/[5\ln(2+\sqrt{3})] \approx 1.578$
$\left\{ \begin{array}{l} (s,2)-CRG^{(+) } \\ (s,2D)-CRG^{(++)} \end{array} \right.$	$2\ln 2/p_c^Y \approx 2.1239$	0.6995	1.5934
(s,i)-PRG (i = 2,2D,3)	$2\ln 2/p_c^Y \approx 2.1239$	0.7023	1.5998
(t,3)-PRG	2.0642	0.7263	1.6544
(t,2)-PRG	2.0499	0.7217	1.6440
(t,2D)-PRG	2.0358	0.7057	1.6075

TABLE 3a

method \ p	0.3473...	0.4	0.5	0.6	0.7	0.8	0.9	1.0
(t,2)-CRG	1	0.8160	0.6075	0.4845	0.4030	0.3450	0.3016	0.2679...
(t,3)-CRG	1	0.8161	0.6082	0.4853	0.4035	0.3453	0.3018	0.2679...
(t,2D)-CRG	1	0.8170	0.6100	0.4867	0.4046	0.3459	0.3020	0.2679...
GT	1	0.8225	0.6135	0.4883	0.4052	0.3461	0.3021	0.2679...
(s,3)-CRG	1	0.8245	0.6150	0.4891	0.4056	0.3463	0.3021	0.2679...
(s,i)-CRG (i = 2,2D)	1	0.8246	0.6152	0.4893	0.4057	0.3464	0.3021	0.2679...
(s,i)-PRG (i = 2,2D,3)	1	0.8246	0.6154	0.4894	0.4058	0.3465	0.3022	0.2679...
(t,2D)-PRG	1	0.8280	0.6180	0.4908	0.4065	0.3468	0.3023	0.2679...
(t,2)-PRG	1	0.8289	0.6192	0.4918	0.4072	0.3472	0.3025	0.2679...
(t,3)-PRG	1	0.8293	0.6188	0.4912	0.4068	0.3469	0.3024	0.2679...

TABLE 3b

method \ p		0.6527...	0.70	0.75	0.80	0.85	0.90	0.95	1.0
(t,2)-CRG	1		0.9035	0.8226	0.7563	0.7007	0.6536	0.6128	0.5773...
(t,3)-CRG	1		0.9040	0.8231	0.7567	0.7010	0.6535	0.6126	0.5773...
(t,2D)-CRG	1		0.9042	0.8241	0.7586	0.7033	0.6556	0.6140	0.5773...
GT	1		0.9078	0.8278	0.7612	0.7048	0.6563	0.6143	0.5773...
(s,3)-CRG	1		0.9088	0.8292	0.7622	0.7052	0.6562	0.6140	0.5773...
(s,i)-CRG (i = 2,2D)	1		0.9089	0.8293	0.7626	0.7058	0.6571	0.6146	0.5773...
(s,i)-PRG (i = 2,2D,3)	1		0.9089	0.8294	0.7627	0.7061	0.6572	0.6147	0.5773...
(t,3)-PRG	1		0.9109	0.8322	0.7658	0.7088	0.6593	0.6158	0.5773...
(t,2)-PRG	1		0.9113	0.8325	0.7659	0.7087	0.6591	0.6157	0.5773...
(t,2D)-PRG	1		0.9113	0.8320	0.7648	0.7074	0.6579	0.6150	0.5773

TABLE 4

method	$\lambda_p^{(i)\Delta} = [\lambda_p^{(i)Y}]^{-1} (t_0=1)$	$\lambda_t^{(i)\Delta} = [\lambda_t^{(i)Y}]^{-1} (p=1)$
(r,2)-CRG (r = t,s)	-1.021	-1
(r,2D)-CRG (r = t,s)	$(-1.021)^{-1} \approx -0.979$	-1
(r,3)-CRG (r = t,s)	-1.064	-1.065